Featured Article

The influence of GAPT extraction on synapse loss of APPswe/PS1dE9 transgenic mice via adjusting Bcl-2/Bax balance

Jing Shi[a,1], Xuekai Zhang[a,1], Jingnian Ni[a], Mingqing Wei[a], Ting Li[a], Bingling Zhou[a], Xiawei Liu[a], Liping Zhang[b], Pengwen Wang[c], Jinzhou Tian[a,*], Yongyan Wang[d]

[a]Third Department of Neurology, Dongzhimen Hospital, Beijing University of Chinese Medicine, Beijing, China
[b]Department of Radiology, Dongzhimen Hospital, Beijing University of Chinese Medicine, Beijing, China
[c]Key Laboratory of Chinese Internal Medicine, Ministry of Education, Beijing University of Chinese Medicine, Beijing, China
[d]Institute of Clinical Medicine, China Academy of Chinese Medical Sciences, Beijing, China

Abstract

Introduction: The degeneration of memory-focused synapses play important roles in Alzheimer's disease (AD) pathogenesis, while it is not well known how β amyloid interferes neuron apoptosis and how a herbal combination GAPT influence synapse loss and neuronal apoptosis pathways of APP/PS1 transgenic mice.

Methods: Three-month and six-month APPswe/PS1dE9 transgenic mice were used. Spatial and memory ability were measured by Morris Water Maze, Neuron and synapse number were assessed by electron microscope; Aβ, Bcl-2/Bax were determined by immunohistochemistry and western blot.

Results: APP/PS1 mice not only had increased Aβ accumulation, impaired memory performance, less synapse number, and much more necrosed neurons, but also had significant reduction in the Bcl-2/Bax ratio. However, GAPT and donepezil showed improved memory performance, less Aβ accumulation, increased neuron and synapse number, as well as restored balance of Bcl-2/Bax.

Discussion: GAPT may improve cognitive functions via both reducing Aβ deposition and restoring Bcl-2/Bax balance of neuron.

© 2018 The Authors. Published by Elsevier Inc. on behalf of the Alzheimer's Association. This is an open access article under the CC BY-NC-ND license (http://creativecommons.org/licenses/by-nc-nd/4.0/).

Keywords: Alzheimer's disease; APP/PS1 transgenic mice; Aβ deposition; GAPT; Bcl-2/Bax balance; Neuron apoptosis

1. Introduction

Alzheimer's disease (AD) is the most common type of dementia in people aged more than 65 years, which accounts for 60%–80% of all-cause dementia. It is a neurodegenerative disorder with prominent memory loss and cognitive decline in clinic [1,2], and severe neuronal loss accompanied by amyloid plaques in the cerebral cortex and neurofibrillary tangles in neuron [3,4] in pathology.

Amyloid beta (Aβ) peptide and hyperphosphorylated microtubule-associated protein tau are main culprits for these two pathologic hallmarks. Aβ is generated normally through proteolytic cleavages by the β-secretase and γ-secretase and degraded by Aβ-degrading enzymes [5]. The balance between Aβ generation and degradation thus becomes an important mechanism in Aβ deposition. The β-Site amyloid precursor protein cleaving enzyme-1 upregulation and insulin-degrading enzyme (IDE) downregulation have been found to play a key role in the overproduction/accumulation of Aβ [6].

Because the very initial symptom of AD almost solely includes severely dysfunctional memory, the degeneration of memory-focused synapses particularly plays an important role in AD pathogenesis [7–9]. Moreover, synapse loss has

been found to be the best correlate of dementia severity [10]. Recent evidence indicates that synapse degeneration caused by soluble $A\beta_{1-42}$-derived diffusible ligands [11] is the main mechanism that interferes with synaptic plasticity, which acts as gain-of-function ligands that attach to synapses. Synapse loss induced by $A\beta$ remains the possible reason for behavioral deficits observed in Tg2576 mice [12]. However, studies using synaptophysin immunohistochemical staining under light microscopy have not produced consistent findings of synapse loss in Tg2576 mice [13–15].

Many different animal models have been created to mimic AD's etiology and facilitate studies of new therapeutics. Transgenic mouse models with mutations in genes related to AD [16], like *beta-amyloid precursor protein (APP)* [17], *apolipoprotein E (APOE)* [17], *presenilin 1 (PS1)* [18], or *presenilin 2 (PS2)* [19]. Moreover, double transgenics, such as PS1/APP [20] or PS2/APP [21], have been proved to accelerate the development of pathology relative to single transgenics [22]. Mice with both APPswe and PS1dE9 mutant transgenes have been created by coinjection into pronuclei of the two transgene constructs [mouse/human (Mo/Hu) chimeric APP695 harboring the Swedish (*K594M/N595L*) mutation and exon 9 deleted PS1] at a single genomic insertion site resulting in the two transgenes being transmitted as a single Mendelian locus [23]. Early $A\beta$ deposition had been observed at the age of 4 to 6 months [24]. Previous animal study showed $A\beta$ deposition occurs from 4 months and with a progressive increase in the plaque number up to 12 months and a similar increase in $A\beta$ levels. Microscopy detection of $A\beta$ deposition and plaques at weekly intervals showed an increase in the *Cornu Ammonis* areas [22], which confirms the utility of double transgenics for studies of biochemical and pathologic mechanisms underlying $A\beta$ deposition, as well as exploring new therapeutic treatments. However, detailed mechanisms about how $A\beta$ deposition interferes neuron apoptosis signals like Bcl-2 and Bax in APP/PS1 transgenic mice are not well studied.

GAPT, also called as GEPT in our previous articles, is a combination of several herbal extracts, consisting of eight active components pro rata of ginsenoside from ginseng, volatile oil and asarone from acorus tatarinowii schott, tenuifolin from polygala, flavonoid glycoside from epimedium, curcumine from tuber curcuma, and others [25–27]. Previous researches have shown that it can markedly enhance spatial learning and memory abilities via reducing GSK3β as well as increasing protein phosphatases 1 and protein phosphatases 2A in streptozocin rat model [25] and reducing $A\beta$ level through inhibiting PS1 activity and promoting IDE and neprilysin activity [26], and protecting synapses through increase in the expression of synaptophysin in APPV717I transgenic mice [27]. A previous clinical study of GAPT in the treatment of amnestic mild cognitive impairment (MCI) showed that GAPT significantly ameliorated the cognitive function of patients with amnestic MCI, an intermediate state of cognitive function before AD [28]. However, it is not known whether GAPT can influence $A\beta$ downstream mechanism in APP/PS1 mice. Therefore, present study aims to investigate the effect of GAPT extract on the expression of $A\beta$ protein and $A\beta$-related neuronal apoptosis enzymes of APP/PS1 transgenic mice.

2. Materials and methods

2.1. Animals

Fifteen 3-month-old and 15 6-month-old APPswe/PS1dE9 transgenic mice were randomly divided, respectively, into five groups, namely model group (M), GAPT low-dose (Gl) group, GAPT medium-dose (Gm) group, GAPT high-dose (Gh) group, and donepezil group. Three same age wild-type C57 mice were used as normal control subjects (nontransgenic inbred mice as normal control subjects) (Permit No. SCXK (Jing) 2009-0004). All animals were provided by the Institute of Experimental Animals, Chinese Academy of Medical Sciences, and Peking Union Medical College (Beijing, China). Ideally, littermates from the same colony should serve as the absolute control. However, in cases when littermates are not available from the provider, the use of C57/BL6J wild-type mice is well accepted as the control for APPswe/PS1dE9 transgenic mice [29,30]. All animals were housed in the Barrier Environment Animal Laboratory of Dongzhimen Hospital (Permit No. SYXK (Jing) 2009-0028). All experimental procedures were performed in compliance with the Provision and General Recommendations of the National Institutes of Health Guide for the Care and Use of Laboratory Animals and were approved by the Animal Research Ethics Board of Beijing University of Chinese Medicine. To represent the whole population, both male and female mice (1:1) were chosen. They were cultivated in a temperature and humidity-controlled (24°C, 40%–70%) pathogen-free vivarium, on a 12:12-hour light–dark cycle (12-hour light [06:00–18:00], 12-hour dark [18:00–06:00]) with free access to food and water.

2.2. Medicine preparation

GAPT consists of eight active components pro rata of ginsenoside from ginseng, volatile oil and asarone from acorus tatarinowii schott, flavonoid glycoside from epimedium, tenuifolin from polygala, curcumine from tuber curcuma, and others [26]. It was provided by Henan Wanxi Pharmaceutical Company Limited (batch no. 20010923, China). Hydrochloric acid donepezil tablets were provided by Eisai Pharmaceutical Company Limited (batch no. 090508A, China). GAPT was dissolved in 0.5% carboxymethyl cellulose (CMC) (Sigma, St. Louis, Missouri, USA) at a concentration of 7.5, 15, and 30 mg/mL, and donepezil tablets were crushed and dissolved in 0.5% CMC at a concentration of 0.092 mg/mL.

2.3. Medicine administration

After 1 week of acclimation to the new environment, the experiment started when the mice were exactly 3 months old. Fifteen 6-month-old and 15 3-month-old APPswe/PS1dE9 double transgenic mice were randomly divided into five groups, respectively ($n = 3$ per group). Six-month-old mice were treated for 3 months, named as short-treatment-period (STP) group. And 3-month-old mice were treated for 6 months, named as long-treatment-period (LTP) group, two groups of wild-type C57/BL6J mice also began to receive intragastrically administrated vehicle at 3- and 6-month old comparatively ($n = 3$ per group). APPswe/PS1dE9 double transgenic mice were used in the other five groups: model group were given 0.5% CMC and donepezil group were given donepezil (APP/PS1 + D; 0.92 mg/kg/d). GAPT was administered at three dosage levels, with a separate group for each: low-dose group (APP/PS1 + Gl; 0.075 g/kg/d), medium-dose group (APP/PS1 + Gm; 0.15 g/kg/d), and high-dose group (APP/PS1 + Gh; 0.30 g/kg/d). C57/BL6J mice served as normal control subjects and were given 0.5% CMC (Fig. 1).

2.4. Behavioral assessment

Spatial learning and memory ability of all mice were measured by orientation navigation tests and spatial probe tests with Morris water maze (MWM) [31] at the end of treatment. The MWM platform for mice (XR-XM101) was purchased from Shanghai Mobile Datum Information Technology (Shanghai, China), which includes a circular pool (120 cm in diameter) with a black-painted sidewall, a moveable hidden plexiglass platform (5 cm in diameter), and a video camera placed above the center of the pool with connection to a computer with tracking software. The MWM process was conducted in a soundproof room without direct light. All animals were pretrained two trials per day for two consecutive days and tested on the third

succeeding day. The pool was filled with water 20 cm deep (water temperature was set to 21°C ± 2°C), and the escape platform was placed 1 cm below the water surface in quadrant two.

Each trial began by placing the mice in one of four arbitrarily defined quadrants, facing the wall, and allowing it to swim freely in the pool. For those who did not reach the platform in 120 seconds, they were placed on the escape platform for 10 seconds to set their memory. The distance and amount of time spent swimming to the platform were recorded. In the test period, no assistance was given to mice that failed to reach the platform. If the animal could not locate the platform in 120 seconds, then it was recorded as 120 seconds. On day 6, a post-training probe trial was conducted with the submerged escape platform removed from the pool. Each mouse was placed into the quadrant opposite to the quadrant that formerly contained the platform in acquisition testing. The animal's swim path and number of annulus crossings were recorded by a computerized tracking system; the percent of time spent in each quadrant and average swim speed were determined. Spatial learning of the mice was evaluated by calculating both the time and the distance to reach the platform. Search strategies were defined accordingly as following. If the animal spent more than 70% of the time traveling within a specified distance of the median line (the line between the animal entry point and the platform; in this case, 15% of the length of the radius of the swimming pool), then the search strategy was defined as a linear pattern. The tendency pattern was defined similarly to the linear pattern except that the designated area was expanded to a distance of up to 50% of the radius of the swimming pool. For the peripheral pattern, the central point of the animal's travel area was first determined. With this point as the center of the circle and 75% of the radius of the swimming pool were calculated the circle's boundary. If the animal spent more than
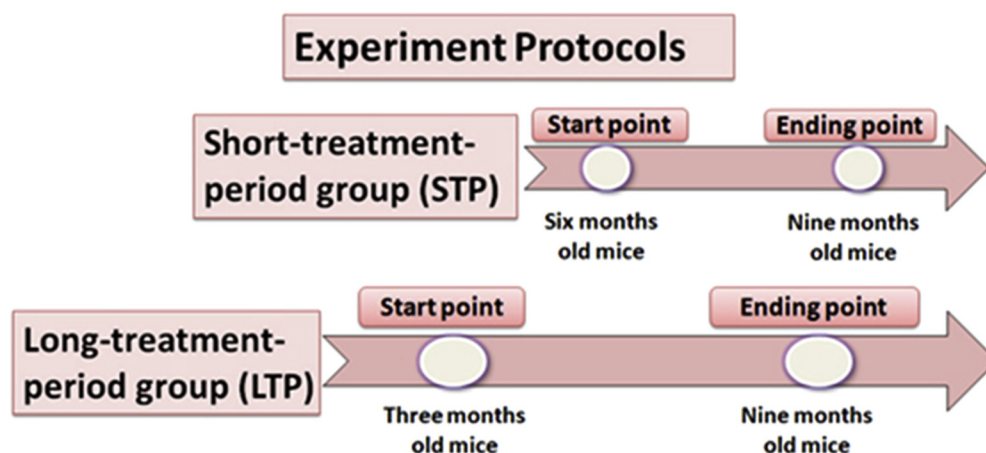

Fig. 1. Flowchart of experimental protocols. Six-month-old mice were treated for 3 months, named as short-treatment-period group, and 3-month-old mice were treated for 6 months, named as long-treatment-period group.

70% of the time traveling outside this boundary, then the search pattern was defined as a peripheral pattern [32].

2.5. Tissue preparation

Three mice of each group were deeply anesthetized with tribromoethanol (500 mg/kg; Sigma-Aldrich, China) and pericardially perfused with heparinized 0.9% saline before removal of the brain. Brains were immersion-fixed in 4% paraformaldehyde (Sun Biomedical Technology Co, Ltd, China) overnight at 4°C and then processed in a phosphate-buffered saline (PBS) solution containing 30% sucrose. Seven days later, brains were embedded in paraffin. Serial coronal sections of the brain were cut at 4-μm intervals for immunohistochemistry staining. The brains of another six arbitrarily selected mice in each group were separated according to regions and homogenate with brain tissue lysis buffer (Loogene Biotechnology Co, Ltd, China) using a small pestle on ice, at a ratio of 1:10 (wt/vol) for 2 minutes, and incubated on ice for 30 minutes. Homogenates were centrifuged at 4300g at 4°C for 30 minutes, and supernatants were collected. The level of protein in the supernatants was determined by the modified Bradford method with Coomassie Brilliant Blue G-250 (Nanjing Jiancheng Bioengineering Institute, China) [33]. Loading buffer was added to samples at a ratio of 4:1, after which samples were placed in boiling water for 5 minutes and then immediately chilled on ice.

Part of the fresh hippocampus tissues was taken out and each one was cut into 1 mm^3 tissue blocks on ice cubes. The tissue blocks were put into 2% glutaraldehyde fixative for 90 minutes at 4°C until they sank down, then they were washed by 0.01 mmol/L PBS for three times and kept in 0.01 mmol/L PBS at room temperature, then treated in 1% osmium tetroxide, dehydrated in a graded series of ethanol solutions, and flat-embedded in Polybed 812 in an oven at 60°C for 48 to 72 hours. From the embedded sections, sections were photographed under the light microscope and then serially cut into semithin (1-μm thick) sections with a Leica ultramicrotome (EM UC6; Leica Microsystems, Wetzlar, Germany). The semithin sections were stained with 1% toluidine blue in 1% borax, examined under the light microscope, and photographed to locate the area of CA1. Selected semithin sections were resectioned into serial ultrathin sections with a silver-gray interference color, corresponding to a thickness of approximately 60 to 70 nm. The ultrathin sections were collected on formvar-coated single-slot grids stained with uranyl acetate and lead citrate and examined using a transmission electron microscope (JEM-2000EX, JEOL Ltd, Japan) [34].

2.6. Neuron counting and synapse number assessment by electron microscope

The counting of pyramidal neurons (i.e., cells with a visible nucleolus) and synapse (i.e., presynaptic membrane, postsynaptic membrane, or both) number was performed in the pyramidal cell layer of the dorsal CA1 subfield of the hippocampus at a magnification of ×20,000. Ten micrographs were taken randomly per region and case using a JEOL transmission electron microscope, and pyramidal neurons and synapses were counted by an electron microscopy technician without knowing groups.

2.7. Western blot

Western blots were performed based on a previously described method. Briefly, samples were placed in boiling water for 5 minutes and then immediately chilled on ice. Aliquots (10 μL) of each sample and 5 μL of marker (10–170 kDa) were loaded onto 10% acrylamide gels (Sigma-Aldrich Co, LLC, USA) and subjected to sodium dodecyl sulphate - polyacrylamide gel electrophoresis using the Bio-Rad mini-gel system (Bio-Rad, USA). Proteins were then electroblotted onto polyvinylidine difluoride membranes. Membranes were blocked with 5% milk at 4°C overnight, and then incubated with primary antibody (Aβ, 1:200, SC-5399, Santa Cruz; Bcl-2, 1:200, SC-492, Santa Cruz; Bax, 1:200, SC-526, Santa Cruz; β-actin, 1:1000, Proteintech). After three washes with PBS containing 0.5% Tween 20 (PBST) (Sun Biomedical Technology Co, Ltd, China), membranes were incubated at room temperature for 1 h with Goat anti-mouse IgG horseradish peroxidase–conjugated secondary antibody (ZSGB-BIO, China) at 1:5000 on a shaker. After three washes with PBST, blots were developed using Luminol reagent (Pierce Biotechnology, Waltham, MA, USA). Densitometric analysis of the blots was completed using Quantity One software (Total Lab Ltd, UK). Expression of these proteins is shown as target protein-β actin ratio.

2.8. Statistical analysis

All data were analyzed in SPSS 17.0 software (IBM Software, Armonk, NY, USA) and presented as the mean ± standard deviation. For the animal behavior test, Kruskal-Wallis analysis, and post hoc comparisons were done with the Mann-Whitney U test. For immunohisto-chemical staining and Western blot analysis, one-way analysis of variance was used for all group analyses, and post hoc comparisons were made with the least significant difference test. Data were considered statistically significant at $P < .05$. Basically, a data normality test was performed first, which showed that all our data were normally distributed ($P > .05$). In the second step, one-way analysis of variance was performed with descriptive and homogeneity of variance test. If variances were not equal, Brown-Forsythe and Welch tests were performed. The analysis showed that all our data variances were equal. The least significant difference test was then chosen for post hoc multiple comparisons.

Table 1
Spatial learning ability measured by orientation navigation tests and space probe tests in the Morris water maze

Groups	Latency time of D1 (s)	Latency time of D2 (s)	Latency time of D3 (s)	Latency time of D4 (s)	Latency time of D5 (s)
A	53.30 ± 15.45	37.2 ± 20.97*	39.32 ± 19.02†	29.82 ± 20.94*	27.02 ± 17.22*
B	59.28 ± 3.72	49.73 ± 16.73‡	47.65 ± 17.54§	53.10 ± 15.18‡	47.70 ± 18.53‡
C	58.00 ± 9.08	47.39 ± 18.94§	39.56 ± 18.91†	41.83 ± 21.34*‡	42.72 ± 21.14‡
D	59.74 ± 2.05	50.45 ± 16.31‡	47.06 ± 17.11§	43.52 ± 19.57†‡	39.85 ± 21.85†‡
E	58.96 ± 5.86	45.85 ± 20.43§	48.18 ± 18.27‡	41.03 ± 20.37*	34.80 ± 20.71*§
F	56.48 ± 10.87	44.72 ± 19.22†§	40.80 ± 18.6³†	45.50 ± 19.36‡	39.92 ± 19.58‡

NOTE. A: Normal control; B: APP/PS1; C: APP/PS1 + donepezil; D: APP/PS1 + Gl; E: APP/PS1 + Gm; and F: APP/PS1 + Gh.The average escape latencies of normal control mice were significantly decreased from D1 to D5. The average escape latencies were significantly longer in APPswe/PS1dE9 transgenic mice compared with their age-matched normal control mice on D2, D3, D4, and D5. Although, mice treated with GAPT and donepezil all showed decrease in escape latencies on D5, of them APP/PS1 + Gm had a shortest escape latency and followed by APP/PS1 + Gl, APP/PS1 + Gh, and APP/PS1 + donepezil.

*Compare to APP/PS1 mice, $P < .01$.
†Compare to APP/PS1 mice, $P < .05$.
‡Compare to normal control group, $P < .01$.
§Compare to normal control group, $P < .05$.

3. Results

3.1. Effects of GAPT on spatial learning and memory in APPswe/PS1dE9 mice

The average escape latencies of normal control mice were significantly decreased from 53.30 ± 15.45 seconds on day 1 to 27.02 ± 17.22 seconds on day 5. Other groups all showed similar decrease during the 5 days training. However, the average escape latencies were significantly longer in APPswe/PS1dE9 transgenic mice compared with their age-matched normal control mice on days 2 ($P < .01$), 3 ($P < .05$), 4 ($P < .01$), and 5 ($P < .01$). Although, mice treated with GAPT and donepezil all showed decreased in escape latencies on the fifth training day, of them APP/PS1 + Gm had a shortest escape latencies with 34.80 ± 20.71 seconds, as followed by APP/PS1 + Gl with 39.85 ± 21.85 seconds, and APP/PS1 + Gh with

39.92 ± 19.58 seconds, and APP/PS1 + donepezil with 42.72 ± 21.14 seconds, respectively, compared with APP/PS1 mice alone ($P < .01$, $P < .05$, $P > .01$, $P > .01$). Detailed data are shown in Table 1, and its sequential change is shown in Fig. 2.

Representative searching strategies include linear type, random type, tendency typs and peripheral type (Fig. 3). The tendency and linear type searching patterns in each group tend to increase from day 1 to day 5, whereas peripheral and random types tend to decrease. However, there were significant less tendency and linear type searching patterns in the APP/PS1 group compared with the normal control group on day 5. Although, tendency and linear type searching patterns were significantly increased in donepezil Gl- and Gh-treated groups. Detailed data are shown in Table 2.

3.2. Effects of GAPT on neurons and synapses in the hippocampal CA1 in APP/PS1 transgenic mice

The neurons of hippocampus CA1 area in the model mice were degenerated, shrank, and necrosed. Their nucleuses were out of the normal shape and chromatin pyknosed and cell organelles were swelling without clear structures. However, the neuron structures of the GAPT- and donepezil-treated mice were similar to the normal control group, except for the low-dosage GAPT group of STP group (Fig. 4).

The counted synapse numbers show that under the same area, the synapse number in the model group is significantly lower than the normal control group. The synapse numbers of Gl, Gm, and Gh of both STP and LTP groups and donepezil LTP groups are all significantly increased without dose-dependency, and when compared with the same GAPT dosage groups of STP and LTP, the synapse number of the LTP group is significantly higher than that of the STP group (see Figs. 5 and 6).
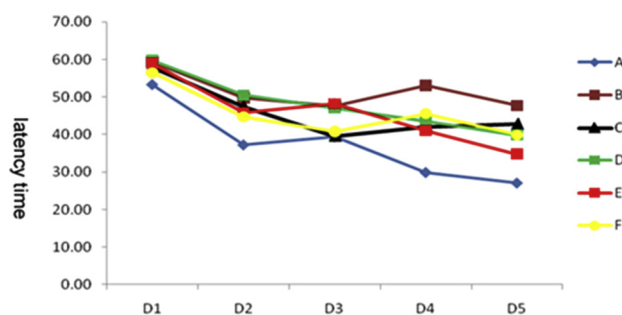

Fig. 2. Spatial learning and memory tests of each group in the Morris water maze. (A) Normal control; (B) APP/PS1; (C) APP/PS1 + donepezil; (D) APP/PS1 + Gl; (E) APP/PS1 + Gm; and (F) APP/PS1 + Gh. The average escape latencies of normal control mice were significantly decreased from day 1 to day 5. The average escape latencies were significantly longer in APPswe/PS1dE9 transgenic mice compared with their age-matched normal control mice. Although mice treated with GAPT and donepezil all showed decrease in escape latencies on the fifth training day, of them APP/PS1 + Gm had a shortest escape latency. Abbreviations: Gh, high-dose group; Gl, low-dose group; Gm, medium-dose group; PS1, presenilin 1.
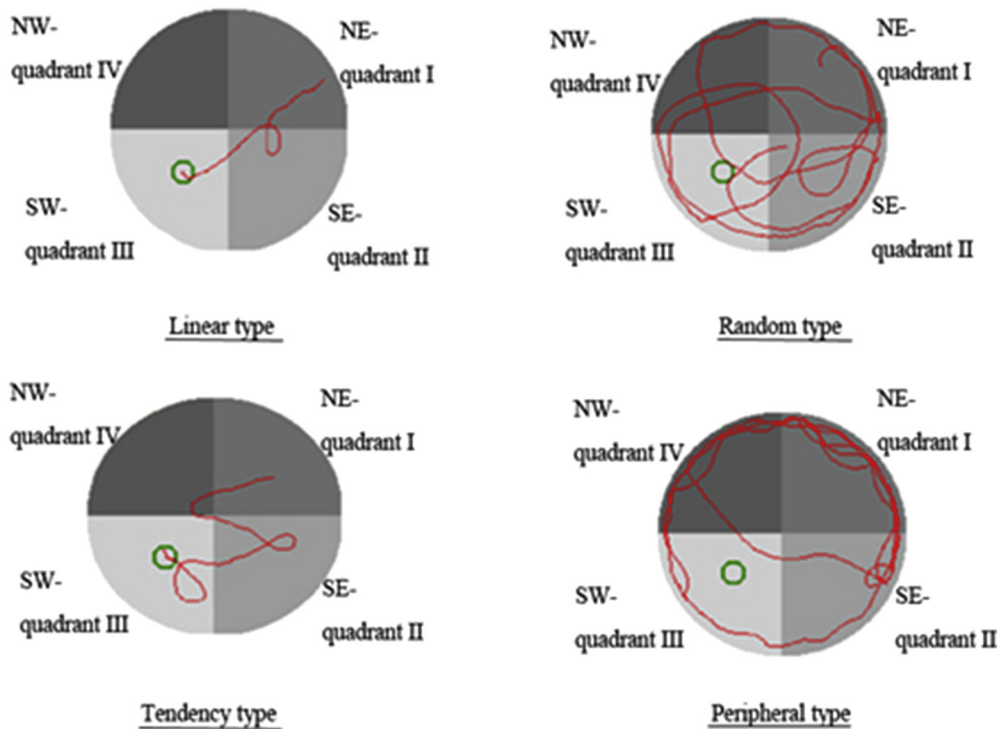
Fig. 3. Representative searching strategies. If the animal spent more than 70% of the time traveling within a specified distance of the median line, then the search strategy was defined as a linear pattern. The tendency pattern was defined similarly to the linear pattern except that the designated area was expanded to a distance of up to 50% of the radius of the swimming pool. For the peripheral pattern, the central point of the animal's travel area was first determined. With this point as the center of the circle and 75% of the radius of the swimming pool determined the circle's boundary. If the animal spent more than 70% of the time traveling outside this boundary, then the search pattern was defined as a peripheral pattern.

3.3. Effect of GAPT on hippocampal Aβ expression in APPswe/PS1dE9 mice

Aβ plaque accumulation is detected in the hippocampus and cortex, as indicated by the brown and yellow staining in the extracellular space (Fig. 7). There are obviously more positively stained plaques in the model group compared with the normal control group, whereas less in the other groups in both STP and LTP. More accurate Aβ expressions were determined by Western blot (Fig. 8).

Western blot analysis showed that significantly more total Aβ was expressed in the APP/PS1 group than in the normal control mice ($P < .01$) in both STP and LTP. Although, compared with APP/PS1 group, total Aβ expression was lower in all other groups. There were significant decreases in the APP/PS1 + donepezil ($P < .05$), APP/PS1 + Gl ($P < .05$), APP/PS1 + Gm ($P < .05$), and APP/PS1 + Gh ($P < .01$) in the STP group, and there were significant decreases in the APP/PS1 + donepezil ($P < .01$), APP/PS1 + Gm ($P < .01$), and APP/PS1 + Gh ($P < .01$) in the LTP group.

3.4. Potential antiapoptotic activity of GAPT by increasing the Bcl-2/Bax ratio in APP/PS1 mice

The expression of apoptotic proteins, including Bcl-2 and Bax was detected by Western blot analysis (Fig. 9). Compared with the normal control group, there was a significant decrease in the Bcl-2/Bax ratio ($P < .01$) in APP/PS1 mice. These results are consistent with the result of ultrastructure of the hippocampus of APP/PS1 mice. In the GAPT-treated group, the Bcl-2/Bax ratio significantly increased in the APP/PS1 + Gl ($P < .05$), APP/PS1 + Gm ($P < .01$), and APP/PS1 + Gh ($P < .01$) in the LTP group. These results suggest that GAPT might
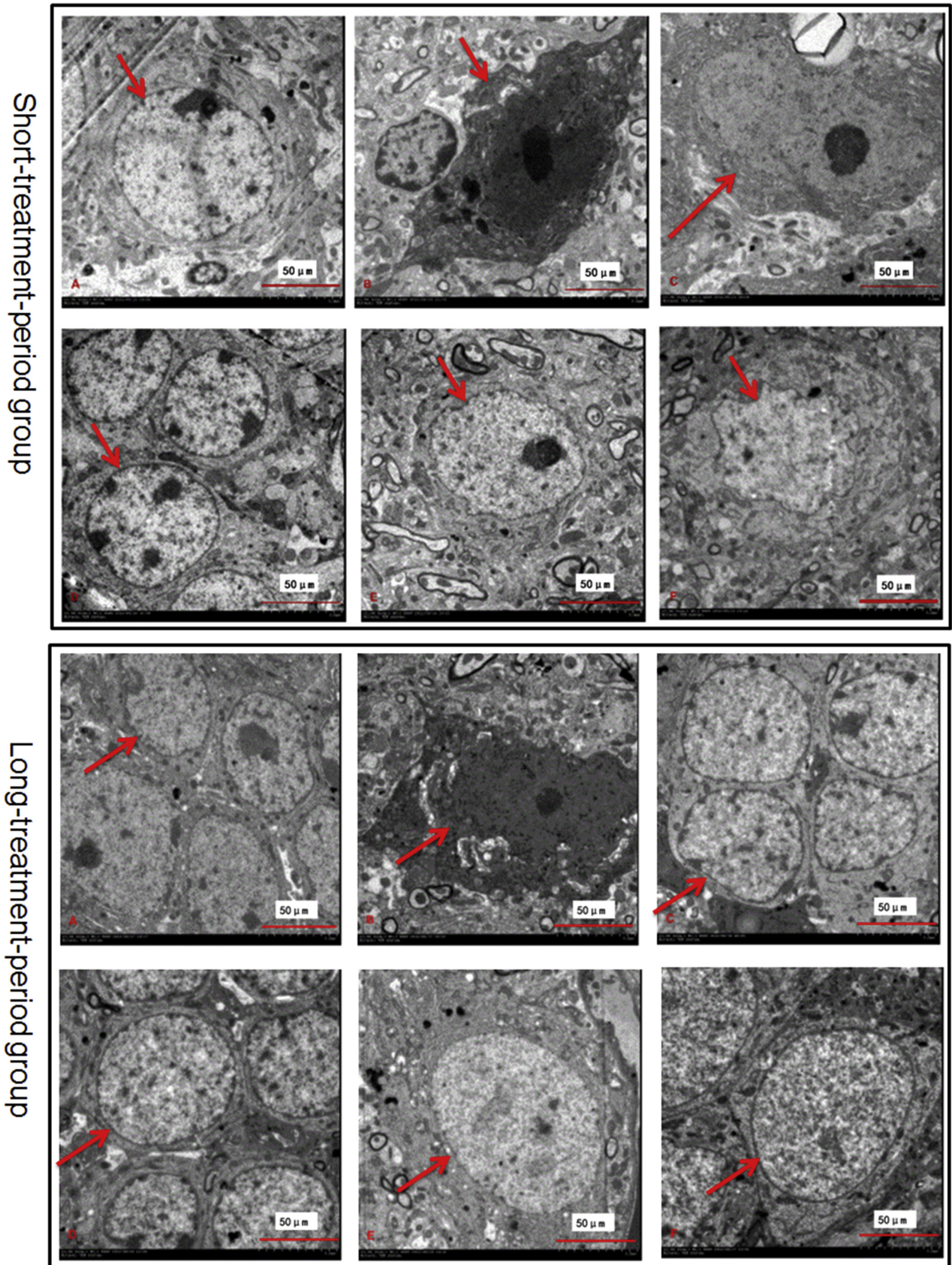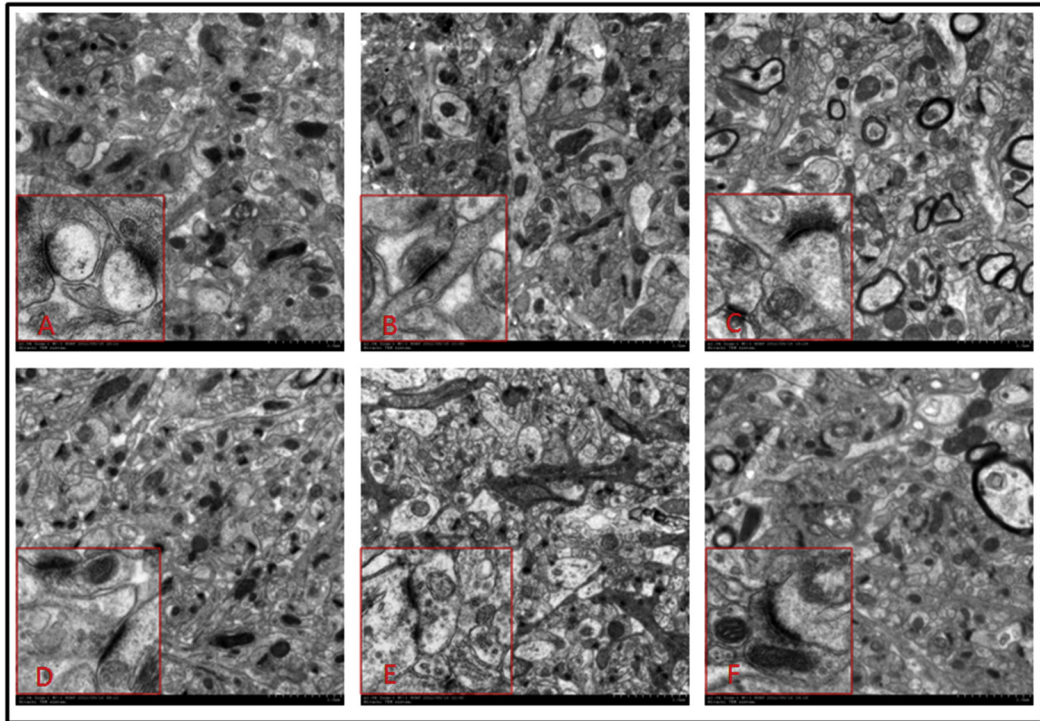
Table 2
Searching patterns of each group

| | Day 1 | | Day 5 | |
Groups	Tendency and linear types	Peripheral and random types	Tendency and linear types	Peripheral and random types
Normal	19	42	51*	10
APP/PS1	9	51	22	38
APP/PS1 + donepezil	7	47	31[†]	23
APP/PS1 + Gl	2	53	25[†]	30
APP/PS1 + Gm	3	45	26	22
APP/PS1 + Gh	10	50	34[†]	26

*Compare to APP/PS1 group, $P < .01$.
[†]Compare to normal group, $P < .05$.

Fig. 4. Ultrastructure of neurons in each group. Pyramidal cell layer of the dorsal CA1 subfield of the hippocampus at a magnification of ×20,000 were taken by a JEOL transmission electron microscope. The normal neuron structure of hippocampus CA1 area (A) and the degenerated, shrank, and necrosed neuron (B and C). Their nucleuses were out of normal shape and chromatin pyknosed and cell organelles were swelling witthout clear structures. The relative normal neuron structure of hippocampus CA1 area (D, E, F). Their nucleuses were relatively normal compare to A or B.

Synapse number of each group

| Groups	Picture No. (N)	Synapse number ($\bar{z} \pm s$)
Normal group	35	16.60±4.195
APP/PS1 group	38	9.76±5.683▲▲
APP/PS1+Gl group	43	13.93±4.032*
APP/PS1+Gm group	48	14.08±5.018**
APP/PS1+Gh group	38	13.89±3.359*
APP/PS1+Donepezil group	30	13.63±3.774
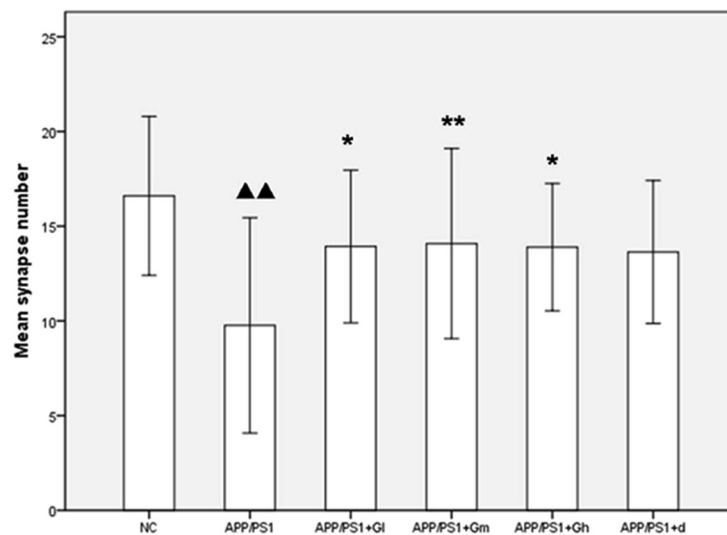
Fig. 5. Ultrastructure of neuron synapses in each group in short-term treatment. The synapses were also taken by the JEOL transmission electron microscope. The synapse number of the model group is significantly lower than the normal control group. There were less synapses in B than in A, while there were more synapses in C, D, E than in B. And the synapse number in F was similar in B. From the table and bar chart, it is clear that the synapse numbers of Gl, Gm, and Gh of both STP and LTP groups and donepezil LTP groups are all significantly increased without dose-dependency. Abbreviations: Gh, high-dose group; Gl, low-dose group; Gm, medium-dose group; LTP, long treatment period; STP, short treatment period. ▲▲Compare to normal group, $P < .01$; *compare to APP/PS1 group, $P < .05$; **compare to APP/PS1 group, $P < .01$.

Ultra-structure of synapses
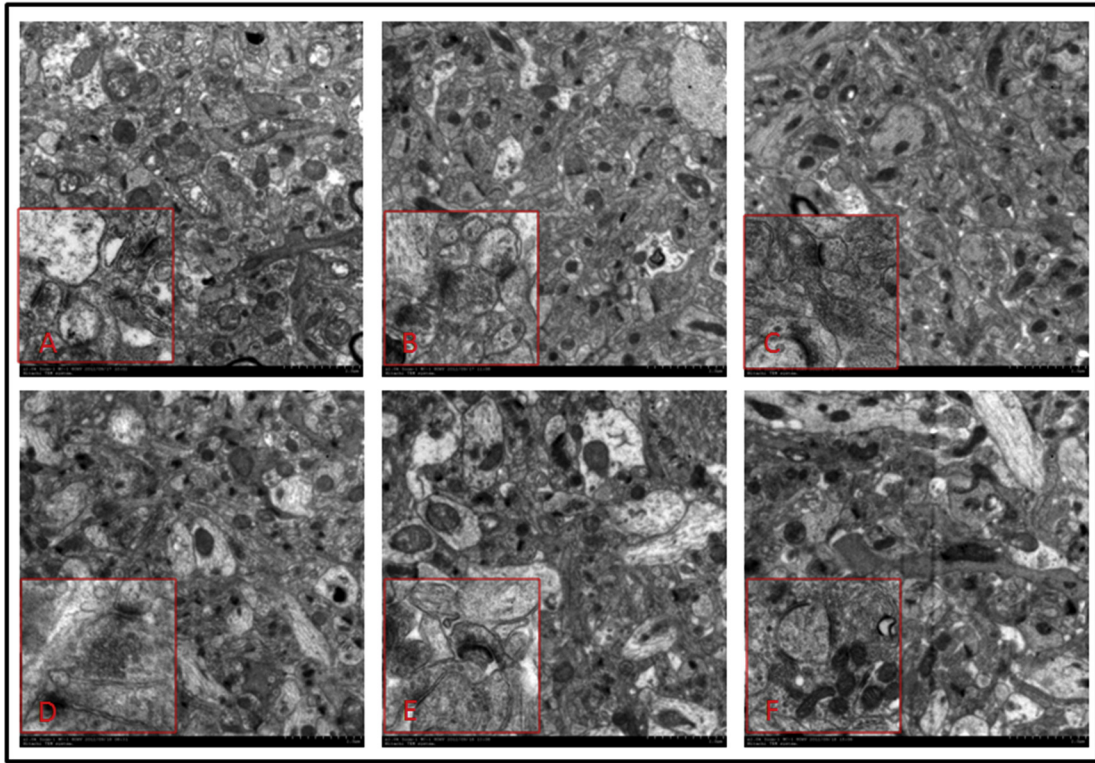
Synapse number of each group

Groups	Picture No. (N)	Synapse number ($\bar{x} \pm s$)
Normal group	30	18.00 ± 4.291
APP/PS1 group	30	10.40 ± 2.541 ▲▲
APP/PS1+Gl group	30	16.70 ± 4.692 **
APP/PS1+Gm group	31	17.32 ± 5.042 **
APP/PS1+Gh group	31	15.61 ± 3.273 **
APP/PS1+Donepezil group	31	16.42 ± 5.169 **
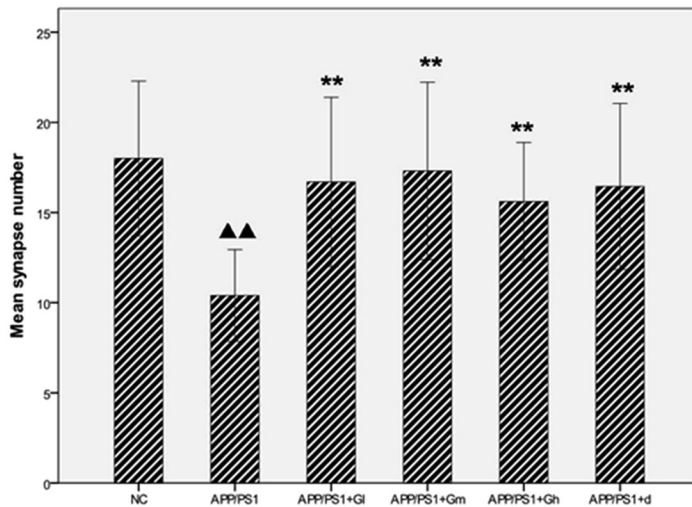
Fig. 6. Ultrastructure of neuron synapses in each group in long-term treatment. The synapses were also taken by the JEOL transmission electron microscope. There were less synapses in B than in A, while there were more synapses in C, D, E than in B. And the synapse number in F was similar in B. And the structure of synapses in B and F were also immature. From the table and bar chart, it is clear that the synapse number of the model group is significantly lower than the normal control group. The synapse numbers of Gl, Gm, and Gh of both STP and LTP groups and donepezil LTP groups are all significantly increased without dose-dependency. Abbreviations: Gh, high-dose group; Gl, low-dose group; Gm, medium-dose group; LTP, long treatment period; STP, short treatment period. ▲▲Compare to normal group, $P < .01$; **compare to APP/PS1 group, $P < .01$.
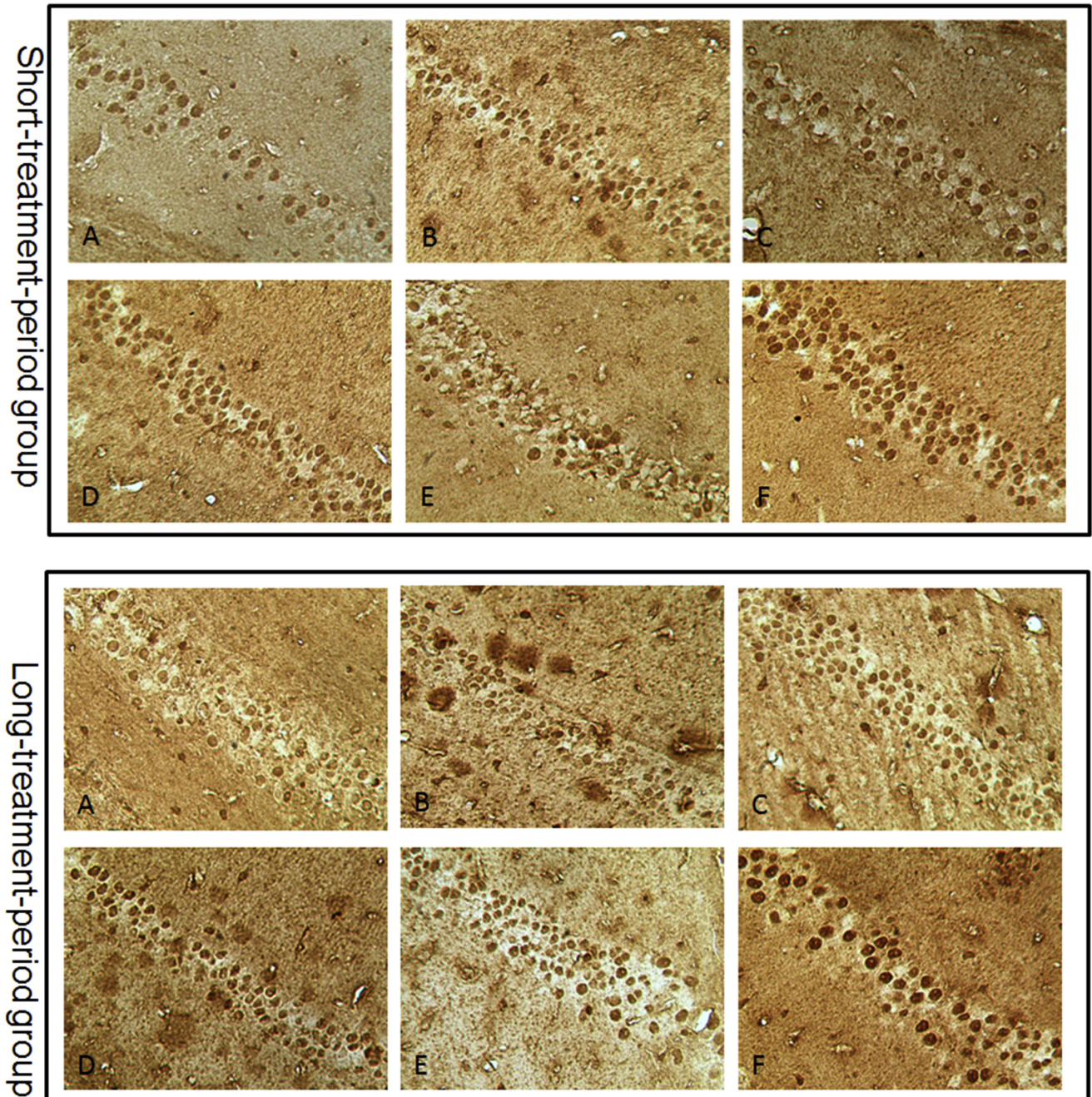
Fig. 7. Amyloid beta (Aβ) plaque accumulation detected by immunohistochemistry in each group. Aβ plaque accumulation as indicated by brown and yellow staining in the extracellular space. There are obviously more positively stained plaques in (B) compared with (A), whereas less in (C, D, E, and F).The color version of this figure is available in the online edition.

have potential antiapoptotic activity on neurons by increasing the Bcl-2/Bax ratio.

4. Discussion

Our previous studies showed that GAPT improved cognitive deficit in both experimental animals and human beings. GAPT has been shown to markedly enhance the function of learning and memory of AD rat model induced by Aβ(1–42) peptide and to significantly improve the spatial learning and memory of APPV717I transgenic mice during the 8 months of treatment [26,35]. It has also been shown that GAPT extracts can reduce levels of endogenous Aβ peptide in the brain of APPV717I transgenic mice via the inhibition of PS1 activity rather than β-Site amyloid precursor protein cleaving enzyme-1 and the promotion of IDE and neprilysin activity [27]. Previous preliminary clinical study also indicated that 3 months of treatment with GAPT had significant effectiveness in improving memory and cognitive impairment and delaying memory
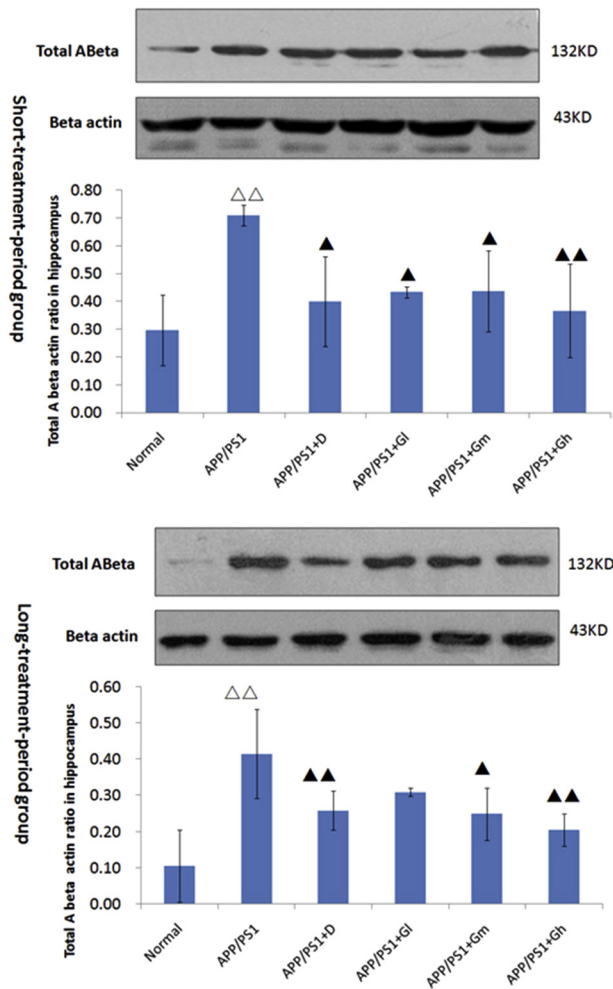
Fig. 8. Amyloid beta (Aβ) accumulation detected by Western blot in each group. Western blot analysis showed that significantly more total Aβ was expressed in the APP/PS1 group than in the normal control mice. When compared with the APP/PS1 group, total Aβ expression was lower in all other groups. △△Compare to normal group, $P < .01$; ▲compare to APP/PS1 group, $P < .05$; ▲▲compare to APP/PS1 group, $P < .01$.
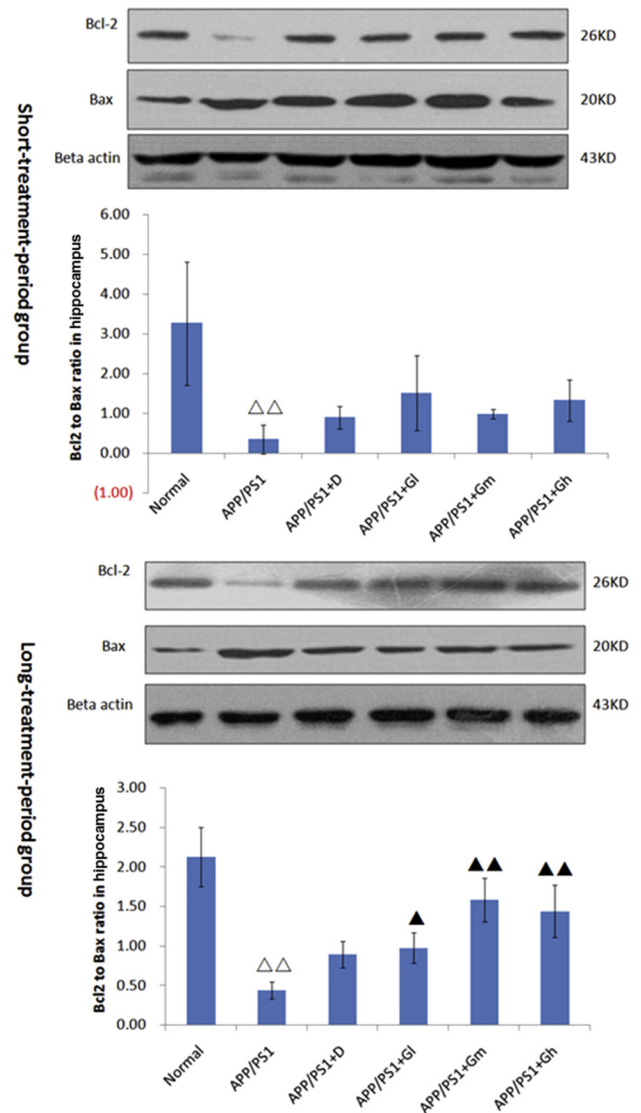

Fig. 9. Bcl-2/Bax ratio detected by Western blot in each group. There was a significant decrease in the Bcl-2/Bax ratio in APP/PS1 mice whereas the Bcl-2/Bax ratio was significantly increased in GAPT-treated groups. △△Compare to normal group, $P < .01$; ▲compare to APP/PS1 group, $P < .05$; ▲▲compare to APP/PS1 group, $P < .01$.

decline through 1 year in 70 patients with amenistic MCI [28]. In this study, the results demonstrated that preventive treatment with GAPT for 6 months adjusted Bcl-2/Bax ratio and prevented neuronal loss and synapses impairment in the hippocampus of APP/PS1 mice.

In the present study, APP/PS1 mouse model was applied to investigate the beneficial effects of GAPT. This transgenic mouse model harbors APP and PS1 gene mutations and offer a powerful animal model with markedly Aβ burden to study the Aβ pathogenesis of AD and to explore the new therapeutic strategy for this disease [36]. Compared with single transgenic for APP or PS1 mutation mice, mice carrying both APP Swedish mutation and PS1-A246E mutation are developed as a model of AD with more severe pathology. They develop large numbers of Aβ deposits in cerebral cortex and hippocampus much earlier than age-matched mice expressing the APP or PS1 mutation alone [37]. In addition to the early appearance of Aβ

deposition in APP/PS1 mouse brain, APP/PS1 mouse developed many other facets of AD neuropathology, such as tau hyperphosphorylation, neuron loss in hippocampus, changes in neurotrophins, deficit in synaptic transmission, changes in behavior, and deficits in lone-term potentiation [38].

APP/PS1 mice have been reported to show brain atrophy and substantial cell loss by as early as at the age of 6 months [38], and a severe hippocampal cell loss (50%) has been reported at the age of 10 months [39]. In our study, we found that APP/PS1 mice displayed a significant decrease in hippocampal neurons at the age of 9 months by electronic scope. Compared with normal control mice, there were significant changes in the ratio of Bcl-2/Bax in the APP/PS1 mouse hippocampus. Previous studies showed that GAPT

attenuated impairment of learning and memory in AD rat model that induced by Aβ(1–42) peptide and APPV717I transgenic mice during the 8 months of treatment with reduced levels of endogenous Aβ peptide in the brain, which was presumed as via the inhibition of PS1 activity rather than β-Site amyloid precursor protein cleaving enzyme-1 and the promotion of IDE and neprilysin activity [26]. The present results suggested that GAPT-induced memory improvement may also related to reducing neuronal apoptosis and protecting synapses of APP/PS1 mice.

5. Conclusion

The main finding of this study is that GAPT reduced Aβ deposition and adjusted apoptosis pathway of neuron and improved memory function. Such effects might partly explain the persistent improvement in cognitive functions in APP/PS1 mouse model following preventive treatment. Because AD is a multifactorial disease with complicated pathogenesis, exploring the multitargets of GAPT might not only find out the detailed mechanisms of it but also may find other innovative and perspective therapy strategies. Considering that GAPT showed several potentially beneficial effects on neurodegeneration processes, together with the ability to decrease Aβ production, adjust the apoptosis of neurons, and protect synapses, it may be well proved as a potential therapeutic agent in long-term AD therapy.

RESEARCH IN CONTEXT

1. Systematic review: Alzheimer's disease (AD), the most common type of dementia in senior people, is clinically characterized by a progressive memory loss and cognitive decline and histopathologically characterized by neuronal loss, amyloid plaques, and neurofibrillary tangles. Because the very initial symptom of AD almost solely comprises severely dysfunctional memory, the degeneration of memory-focused synapses particularly plays an important role in AD pathogenesis. Although early amyloid beta (Aβ) deposition had been observed in APP/PS1 transgenic mice at an age of 4 to 6 months, it is not well known how Aβ deposition interferes neuron apoptosis signals like Bcl-2 and Bax in APP/PS1 mice. The present study aimed to find out the relationship among Aβ deposition, synapse loss, and Bcl-2 as well as Bax. Meanwhile, GAPT used as a combination of herbal extracts consisting of extracts from ginseng, polygala, acorus tatarinowii schott, tuber curcuma, and others in the present study has been found to enhance markedly memory abilities in both AD animal models and patients with mild cognitive impairment or AD. The present study was also aimed to investigate the preventive and therapeutic effects of GAPT on synapse loss and Bcl-2/Bax balance induced by Aβ deposition.

2. Interpretation: We found that APP/PS1 mice not only had increased Aβ plaque accumulation, impaired memory performance, less synapse number, and much more necrosed neurons in hippocampus CA1 area, but also had significant decrease in the Bcl-2/Bax ratio in the hippocampus. However, the APP/PS1 mice treated with GAPT and donepezil showed improved memory performance, less of the Aβ plaque accumulation, better neuron structure, and increased synapse number, as well as restored balance of Bcl-2/Bax in the hippocampus. Thus, GAPT may improve cognitive functions via both reducing Aβ deposition and restoring Bcl-2/Bax balance of neuron.

3. Future directions: We think this finding not only elucidates detailed mechanisms of Aβ plaque accumulation, impaired memory performance, synaptic loss, necrosed neurons in hippocampus CA1 area and Bcl-2/Bax ratio in APP/PS1 mice, but also provides experimental evidence of using herbal therapy to treat AD.

References

[1] van der Flier WM, Scheltens P. Epidemiology and risk factors of dementia. J Neurol Neurosurg Psychiatry 2005;76:v2–7.

[2] Querfurth HW, Laferla FM. Alzheimer's disease. N Engl J Med 2010; 362:329–44.

[3] Selkoe DJ. Alzheimer's disease results from the cerebral accumulation and cytotoxicity of amyloid-beta-protein. J Alzheimers Dis 2001;3:75–80.

[4] Serrano-Pozo A, Frosch MP, Masliah E, Hyman BT. Neuropathological alterations in Alzheimer disease. Cold Spring Harb Perspect Med 2011;3:a006189.

[5] Selkoe DJ. Alzheimer disease: mechanistic understanding predicts novel therapies. Ann Intern Med 2004;140:627–38.

[6] Li R, Lindholm K, Yang L, Yue X, Citron M, Yan R, et al. Amyloid beta peptide load is correlated with increased beta-secretase activity in sporadic Alzheimer's disease patients. Proc Natl Acad Sci U S A 2004;101:3632–7.

[7] Terry RD, Masliah E, Salmon DP, Butters N, DeTeresa R, Hill R, et al. Physical basis of cognitive alterations in Alzheimer's disease: synapse loss is the major correlate of cognitive impairment. Ann Neurol 1991; 30:572–80.

[8] Selkoe DJ. Alzheimer's disease is a synaptic failure. Science 2002; 298:789–91.

[9] Coleman P, Federoff H, Kurlan R. A focus on the synapse for neuroprotection in Alzheimer disease and other dementias. Neurology 2004;63:1155–62.

[10] Sze CI, Troncoso JC, Kawas C, Mouton P, Price DL, Martin LJ. Loss of the presynaptic vesicle protein synaptophysin in hippocampus correlates with cognitive decline in Alzheimer disease. J Neuropathol Exp Neurol 1997;56:933–44.

[11] Lacor PN, Buniel MC, Furlow PW, Clemente AS, Velasco PT, Wood M, et al. Aβ oligomer-induced aberrations in synapse composition, shape, and density provide a molecular basis for loss of connectivity in Alzheimer's disease. J Neurosci 2007;27:796–807.

[12] Stern EA, Bacskai BJ, Hickey GA, Lombardo JA, Hyman BT. Cortical synaptic integration in vivo is disrupted by amyloid-β plaques. J Neurosci 2004;24:4535–40.

[13] King DL, Arendash GW. Behavioral characterization of the Tg2576 transgenic model of Alzheimer's disease through 19 months. Physiol Behav 2002;75:627–42.

[14] Dong H, Martin MV, Chambers S, Csernansky JG. Spatial relationship between synapse loss and β-amyloid deposition in Tg2576 mice. J Comp Neurol 2007;500:311–21.

[15] Spires TL, Meyer-Luehmann M, Stern EA, McLean PJ, Skoch J, Nguyen PT, et al. Dendritic spine abnormalities in amyloid precursor protein transgenic mice demonstrated by gene transfer and intravital multiphoton microscopy. J Neurosci 2005;25:7278–87.

[16] Laferla FM, Green KN. Animal models of Alzheimer disease. Cold Spring Harb Perspect Med 2012;2:a006320.

[17] Kawabata S, Higgins GA, Gordon JW. Amyloid plaques, neurofibrillary tangles and neuronal loss in brains of transgenic mice overexpressing a C-terminal fragment of human amyloid precursor protein. Nature 1991;354:476–8.

[18] Crook R, Verkkoniemi A, Perez-Tur J, Mehta N, Baker M, Houlden H, et al. A variant of Alzheimer's disease with spastic paraparesis and unusual plaques due to deletion of exon 9 of presenilin 1. Nat Med 1998;4:452–5.

[19] Herreman A, Serneels L, Annaert W, Collen D, Schoonjans L, Strooper BD. Total inactivation of gamma-secretase activity in presenilin-deficient embryonic stem cells. Nat Cell Biol 2000; 2:461–2.

[20] Holcomb L, Gordon MN, Mcgowan E, Yu X, Benkovic S, Jantzen P, et al. Accelerated Alzheimer-type phenotype in transgenic mice carrying both mutant amyloid precursor protein and presenilin 1 transgenes. Nat Med 1998;4:97–100.

[21] Richards JG, Higgins GA, Ouagazzal A, Ozmen L, Kew JN, Bohrmann B, et al. PS2APP transgenic mice, coexpressing hPS2mut and hAPPswe, show age-related cognitive deficits associated with discrete brain amyloid deposition and inflammation. J Neurosci 2003;23:8989–9003.

[22] Garcia-Alloza M, Robbins EM, Zhang-Nunes SX, Purcell SM, Betensky RA, Raju S, et al. Characterization of amyloid deposition in the APPswe/PS1dE9 mouse model of Alzheimer disease. Neurobiol Dis 2006;24:516–24.

[23] Jankowsky JL, Slunt HH, Ratovitski T, Jenkins NA, Copeland NG, Borchelt DR, et al. Co-expression of multiple transgenes in mouse CNS: a comparison of strategies. Biomol Eng 2001;17:157–65.

[24] Jankowsky JL, Fadale DJ, Anderson J, Xu GM, Gonzales V, Jenkins NA, et al. Mutant presenilins specifically elevate the levels of the 42 residue beta-amyloid peptide in vivo: evidence for augmentation of a 42-specific gamma secretase. Hum Mol Genet 2004;13:159–70.

[25] Chen YJ, Wang R, Sheng Sl. Effect of Jinsiwei on neuron microtubule in hippocampus and expression of Tan-protein phosphorylation related enzyme in rats with AD. Tianjin J Tradit Chin Med 2008;25:59–62.

[26] Tian J, Shi J, Zhang L, Yin J, Hu Q, Xu Y, et al. GEPT extract reduces Abeta deposition by regulating the balance between production and degradation of Abeta in APPV717I transgenic mice. J Curr Alzheimer Res 2009;6:118–31.

[27] Shi J, Tian J, Zhang X, Wei M, Yin L, Wang P, et al. A combination extract of ginseng, epimedium, polygala, and tuber curcumae increases synaptophysin expression in APPV717I transgenic mice. J Chin Med 2012;7:13.

[28] Tian J, Shi J, Miao Y. A preliminary study of GEPT capsule in the treatment of amnestic mild cognitive impairment. J Alzheimers Dement 2009;5:P255.

[29] Elvang AB, Volbracht C, Pedersen LO, Jensen KG, Karlsson JJ, Larsen SA, et al. Differential effects of gamma-secretase and BACE1 inhibition on brain Abeta levels in vitro and in vivo. J Neurochem 2009;110:1377–87.

[30] Lim JE, Song M, Jin J, Kou J, Pattanayak A, Lalonde R, et al. The effects of MyD88 deficiency on exploratory activity, anxiety, motor coordination, and spatial learning in C57BL/6 and APPswe/PS1dE9 mice. Behav Brain Res 2012;227:36–42.

[31] Morris R. Developments of a water-maze procedure for studying spatial learning in the rat. J Neurosci Methods 1984;11:47–60.

[32] Wang P, Su C, Li R, Wang H, Ren Y, Sun H, et al. Mechanisms and effects of curcumin on spatial learning and memory improvement in APPswe/PS1dE9 mice. J Neurosci Res 2014;92:218–31.

[33] Bradford MM. A rapid and sensitive method for the quantitation of microgram quantities of protein utilizing the principle of protein-dye binding. J Anal Biochem 1976;72:248–54.

[34] Shibuki K, Gomi H, Chen L, Bao S, Kim JJ, Wakatsuki H, et al. Deficient cerebellar long-term depression, impaired eyeblink conditioning, and normal motor coordination in GFAP mutant mice. Neuron 1996;16:587–99.

[35] Shi J, Tian J, Xu Y, Sheng S, Wang Y. Influence of GETO extract on myelin sheath structure and myelin basic protein content in the brain with AD model. J Alzheimers Dement 2006;2:s601.

[36] Bertram L, Tanzi RE. Thirty years of Alzheimer's disease genetics: the implications of systematic meta-analyses. Nat Rev Neurosci 2008; 9:768–78.

[37] Kurt MA, Davies DC, Kidd M, Duff K, Rolph SC, Jennings KH, et al. Neurodegenerative changes associated with β-amyloid deposition in the brains of mice carrying mutant amyloid precursor protein and mutant presenilin-1 transgenes. J Exp Neurol 2001;171:59–71.

[38] Faure A, Verret L, Bozon B, El Tannir El Tayara N, Ly M, Kober F, et al. Impaired neurogenesis, neuronal loss, and brain functional deficits in the APPxPS1-Ki mouse model of Alzheimer's disease. Neurobiol Aging 2011;32:407–18.

[39] Casas C, Sergeant N, Itier J, Blanchard V, Wirths O, der Kolk N, et al. Massive CA1/2 neuronal loss with intraneuronal and N-terminal truncated Aβ42 accumulation in a novel Alzheimer transgenic model. Am J Pathol 2004;165:1289–300.